



6G Industrial Networks: Mobility-Centric Evaluation of Multi-cell mmWave Systems

M. Danger*, C. Arendt*, H. Schippers*, S. Böcker*, N. Beckmann[‡], R. Schmitt[‡], and C. Wietfeld*

*Communication Networks Institute (CNI), TU Dortmund University, 44227 Dortmund, Germany

E-mail: {Marco.Danger, Christian.Arendt, Hendrik.Schippers, Stefan.Boecker, Christian.Wietfeld}@tu-dortmund.de

[‡]Fraunhofer Institute for Production Technology (IPT), 52074 Aachen, Germany

E-mail: {Niklas.Beckmann, Robert.Schmitt}@ipt.fraunhofer.de

Abstract—The adoption of Millimeter-Wave (mmWave) technology in industrial environments presents significant challenges in maintaining consistent Quality of Service (QoS) under dynamic and complex conditions. This study investigates the performance of a multi-cell mmWave network deployed in a large-scale industrial hall, emphasizing the mobility of end devices and their interaction with environmental factors. Measurements were conducted using a Non-Standalone (NSA) 5G network configuration with one sub-6 GHz anchor and two mmWave Radio Units (RUs) deployed for comprehensive coverage. The evaluation highlights key aspects such as Secondary Node (SN) changes, end device orientation, and network load conditions. Results from mobile measurements reveal the influence of device alignment and environmental changes on performance, transmission power and connectivity, particularly in SN change areas. Additionally, the impact of static load generation on multi-cell network performance is examined, demonstrating the interplay between mobility and network capacity. These findings underscore the importance of precise device orientation and environmental awareness in optimizing mmWave deployments.

Index Terms—mmWave communications, indoor measurements, multi-cell, multi-user, mobility.

I. INTRODUCING THE NEED OF MULTI-CELL NETWORKS FOR ROBUST INDUSTRIAL OPERATIONS

The potential for enhancing wireless network performance through the utilization of Millimeter-Wave (mmWave) and Terahertz (THz) frequencies has gained considerable recognition [1]. However, the implementation of this approach in real-world industrial environments has exposed significant challenges. Contrary to controlled test environments, industrial settings are characterized by high dynamism and the presence of unpredictable factors such as interference, obstructions, and variable radio conditions. These factors complicate the full and robust reproduction of the high performance observed under idealized test conditions in larger-scale industrial deployments. In order to leverage the advantages of Frequency Range 2 (FR2) in today's 5G and future 6G networks for a wider range of applications, a sufficient Quality of Service (QoS) must be guaranteed in highly dynamic production environments. To achieve this, the mmWave radio system must be designed more robustly and the channel quality between Radio Units (RUs) and end devices needs to be optimized.

Against this background, this work evaluates the performance of several static and mobile devices within an industrial environment equipped with a Non-Standalone

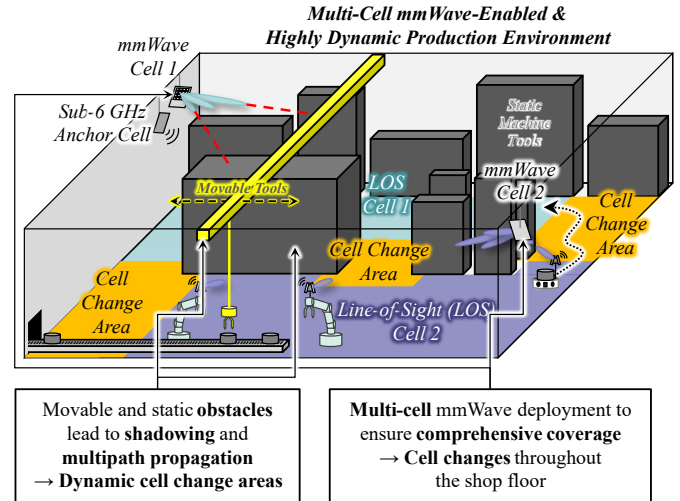


Fig. 1: Multi-cell mmWave network enables widespread coverage yet leads to several Secondary Node (SN) change areas.

(NSA) multi-cell mmWave network. For this purpose, a series of measurements were conducted within a large-scale industrial setting where a network is deployed consisting of one sub-6 GHz anchor and two mmWave RUs placed on opposite walls of the hall. As illustrated in Fig. 1, this scenario includes multiple static and mobile components that impact radio propagation, consequently influencing cell change areas. The multi-cell configuration ensures comprehensive coverage, including regions where Secondary Node (SN) changes occur. These zones are a particular focus of this work, as the multi-cell configuration enables continuous coverage of the radio environment, but the transition from a mmWave RU to another can result in short-term performance degradation, thus offering opportunities for enhancement.

As indicated in previous measurements documented in [2], a single mmWave antenna is inadequate for ensuring a robust FR2 connection in all corridors. The end devices used to obtain these findings are based on the Spatially distributed Traffic and Interference Generation (STING) concept [3] and are likewise utilized for the measurements in this study. With this approach, multiple controllable end devices are deployed throughout a radio environment to generate load, which allows the performance of networks to be tested, and to monitor the performance of the complete system, including

both distributed and centralized networks key performance indicators (KPIs). The measurement results are subsequently processed into a multidimensional performance evaluation and visualized, for example, as Radio Environmental Map (REM). In contrast to the prior study, the present work emphasizes mobility-centric measurements employing the so-called mobile STING, while static STING units can be deployed for additional load generation within the network.

The remainder of this work is structured as follows. In Sec. II, related studies that investigate mmWave networks in more detail are discussed. Next, Sec. III describes the methodology used to carry out the measurements, the results of which are then discussed in Sec. IV. Finally, the findings of this work are summarized in Sec. V and an outlook on future undertakings is given.

II. ASSESSING FEATURES AND PERFORMANCE OF MMWAVE INDOOR NETWORKS

Maintaining robust QoS in mmWave networks is challenging due to high path losses, necessitating the use of multiple cells. The concept of multi-connectivity, as demonstrated in [4], ensures reliable connections by enabling cooperation between the Master Node (MN), SNs and User Equipments (UEs). The technical implementation of such schemes, including SN addition, modification, release, and change, is comprehensively described in the mobile radio standard [5]. In this study's network configuration, the LTE anchor cell serves as the MN, while two separate mmWave cells function as SNs, each with distinct basebands. Consequently, the process of SN changes, initiated by the Mobility Management Entity (MME), is critical to the mobility analysis conducted. This procedure involves several stages: first, the target SN is added based on measurements from both the source and target SNs. Next, the source SN is released, and finally, the UE's connection is reconfigured to the target SN.

The feasibility of deploying mmWave networks in industrial settings has been supported by studies such as [6], which examined their use for industrial robotics applications. However, the authors highlight the necessity of further investigations into load handling, multi-user scenarios, and mobility to comprehensively validate these findings.

Similarly, [7] explored FR2 networks in industrial environments with a particular focus on mobility management. Their findings revealed significant variations in Reference Signal Received Power (RSRP) due to Line-of-Sight (LOS) and Non-Line-of-Sight (NLOS) conditions. The study also tested various thresholds for beam switching, concluding that environment-specific thresholds can optimize network performance. This insight is particularly relevant to the SN changes analyzed in the present work, suggesting a promising direction for improving the robustness of mmWave networks in dynamic industrial settings.

In [8], a mmWave network was also evaluated within an industrial environment, as FR2 frequencies can cover the high demands of various robotics applications. To meet the challenge of blockage and mobile end users, an improved beam

switching criteria was developed. During the experiments carried out for this purpose, it was found that environmental changes have an influence on the beam set used in a cell, which is why the authors consider scenario-specific configurations to be necessary. This finding is supported by the results presented in this work.

Mobility-centric measurements in mmWave networks are also the focus of [9]. In this comprehensive work, the authors discuss several mobility scenarios and models to identify key challenges and oppose them to existing solutions. Lastly, several open issues concerning mobility-aware mmWave communications that deserve further investigation are listed, including heterogeneous mobile networks, which can involve multi-cell configurations, as in the present work.

In [10], a dynamic Unmanned Aerial Vehicle (UAV)-based Reconfigurable Intelligent Surface (RIS) system for multi-cell multi-user communication is investigated. In general, the deployment of intelligent reflectors can improve network performance across complex settings, making this option also relevant for the large-scale industrial environment considered in this work.

The authors in [11] likewise performed an empirical performance evaluation of a mmWave network, whereby the latency measurements performed complement the KPIs of this paper. Furthermore, the authors suggest that multi-cell deployments may be necessary to ensure comprehensive coverage across industrial settings. This assumption is confirmed by the measurement results presented in this paper.

Based on the listed findings of previous research and our prior measurement [2], whose results revealed connectivity issues with a single mmWave RU in the same large-scale industrial environment, in this work mobility analysis is performed in a multi-cell network, investigating UE orientation, the effect of environmental changes, multi-user as well as load scenarios.

TABLE I: Configuration of 5G mmWave multi-cell network and UEs.

	Parameter	Description/Value
Multi-Cell Configuration	1x LTE Anchor Cell	
	Radio Unit	Ericsson Radio 2203
	Frequency Band	LTE band 7 (FDD)
	Center Frequency	2.65 and 2.53 GHz (DL/UL)
	Bandwidth	20 MHz
	Transmit Power	5 W (EIRP)
	2x NR mmWave Cells	
	Radio Unit	Ericsson AIR 1281
	Frequency Band	5G NR n257 (TDD)
	Frequency Range	26.7 to 27.5 GHz
TDD Pattern	DDDSU	
Component Carriers (CCs)	8 (100 MHz each)	
Subcarrier Spacing (SCS)	120 kHz	
Transmit Power	2 W (EIRP)	
User Equipments (UEs)	1x Mobile and 6x Static UEs	
	Device Model	Quectel 5GDM01EK with Quectel RG530F-EU
	Modem	Qualcomm SDX65
	mmWave Antenna Module	RA530T with four QTM547 (8 × 8, cross-polarized)
	LTE Category	Cat 20 / Cat 18 (DL/UL)
	5G NR Compliance	Release 16 NSA/SA
	Power Class	Class 3 (23 dBm)
MIMO Capabilities	FR1: DL 4 × 4, UL 2 × 2 FR2: DL 2 × 2, UL 2 × 2	
Mobile UE LiDAR Sensor	Velodyne VLP-16 Puck LITE	

III. METHODOLOGY FOR EVALUATING MULTI-CELL NETWORKS USING MOBILE AND STATIC DEVICES

This chapter describes the methodology of the measurements performed. In Sec. III-A the network architecture as well as the setup of mobile and static STING units is explained. Subsequently, the measurement scenarios and their parameterization are described in Sec. III-B. Finally, the post-processing of the recorded KPIs is outlined, on the results of which the evaluation of the network performance is based.

A. Network Architecture and STING Unit Setup

The main parameters of the network components and the UEs as part of the measurement system are listed in Tab. I. The multi-cell network consists of one sub-6 GHz anchor cell and two identically configured mmWave RUs which are mounted on opposite walls of the hall, each at a height of 6 m (cf. Fig. 2). In this case, the anchor cell is co-deployed with mmWave RU 1. Within this multi-cell network, one mobile and six static UEs are used as STING units, all based on the same device model and modem. Since their individual mmWave antennas point in only one direction, a detailed study of UE mobility as well as orientation is possible and necessary. While the static units are each mounted on a tripod at a height of 1.5 m, the mobile unit's device is placed on a robotic platform that, thanks to omnidirectional wheels and a LiDAR sensor, can both move freely in all corridors and locate itself after an initial scan. With this setup, it is possible to perform location-based continuous measurements by driving through all accessible aisles at walking speed to generate REMs, which are then used for evaluation.

An additional feature of the radio environment are cranes, four of which are distributed throughout the hall at a height of 5.8 to 6.8 m and can be moved from east to west. During the measurements, one crane was moved due to ongoing operations within the production environment, so two positions for this crane are shown in Fig. 2, marked in orange. The influence of this environmental change on the network performance is part of the evaluation, as the cranes are located at the height of the RUs and thus the propagation of the radio waves can be strongly influenced during some crane positions, which can have an impact on the connectivity of the UEs on the shop floor.

B. Scenarios, Parameterization and Post-processing

The measurements in this work are carried out in two different scenarios:

- Single-User: the mobile STING unit is the only device connected to the given network and can therefore access the maximum resources of both mmWave RUs.
- Multi-Load: while the mobile STING unit moves around the entire shop floor, six static and co-located STING units cause a complete resource utilization of mmWave RU 2 whilst being located at the static STING position, marked in Fig. 2.

In both cases, the mobile STING unit follows the same trajectory: $A - B - C - D - E - D - C - B - F - E -$

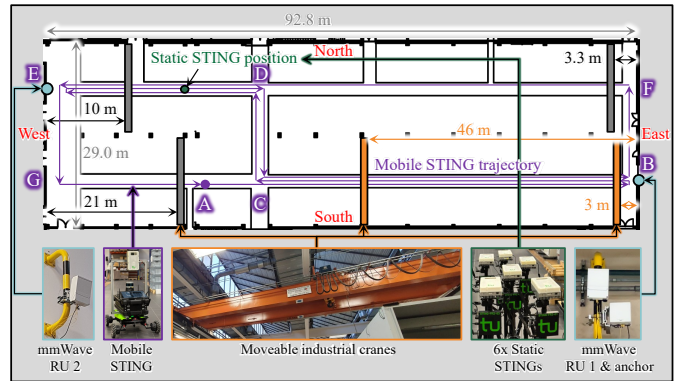


Fig. 2: Floor plan and positioning of static as well as mobile hardware components within dynamic industrial environment.

$G - A$ (cf. Fig. 2). By pursuing this route, all main corridors of the measurement environment are covered and several SN changes are forced. The orientation of the UE on top of the mobile robot can be changed between horizontal (towards the ceiling) and vertical (eastwards), while the static STING units are permanently oriented towards the ceiling in order to detect as many different propagation paths as possible from all cells.

Both the static and mobile units perform one of two active measurements per drive through while monitoring device-specific KPIs (e.g., Synchronization Signal Reference Signal Received Power (SS-RSRP) or New Radio (NR)-Physical Cell ID (PCID)): Uplink (UL) or Downlink (DL) data rate. The throughput measurements via *iperf* [12] are parameterized so that the device-specific maximum data rate (UL: 670 Mbit/s, DL: 2.1 Gbit/s) is permanently queried in both UL and DL directions. With this setting, the maximum capability of the network is requested, allowing its performance to be optimally evaluated and analyzed. At the same time, the effects of variable radio conditions, e.g. introduced by UE alignment or environmental changes, are most evident in comparison to the baseline performance.

All active as well as passive KPIs of the distributed STING units and the mmWave RUs recorded during the execution of the described measurement scenarios are used for subsequent analysis. While the static UEs are co-deployed at a fixed position (cf. Fig. 2), the measured values can be matched with the tracked position of the mobile STING (every 500 to 700 ms) in order to perform location specific analysis in the form of REMs.

IV. MULTI-LAYER PERFORMANCE EVALUATION

Throughout this section, the evaluation of the measurements carried out and the performance of the multi-cell mmWave network is analyzed from three perspectives. Firstly, the performance of a single mobile user is considered in Sec. IV-A to establish the baseline performance and to gain an initial understanding of the SN change areas. The effect of UE alignment and environmental changes on connectivity is then examined in Sec. IV-B. Finally, Sec. IV-C analyzes the effect of multiple simultaneous users in one of the two mmWave cells on the performance of the mobile STING.

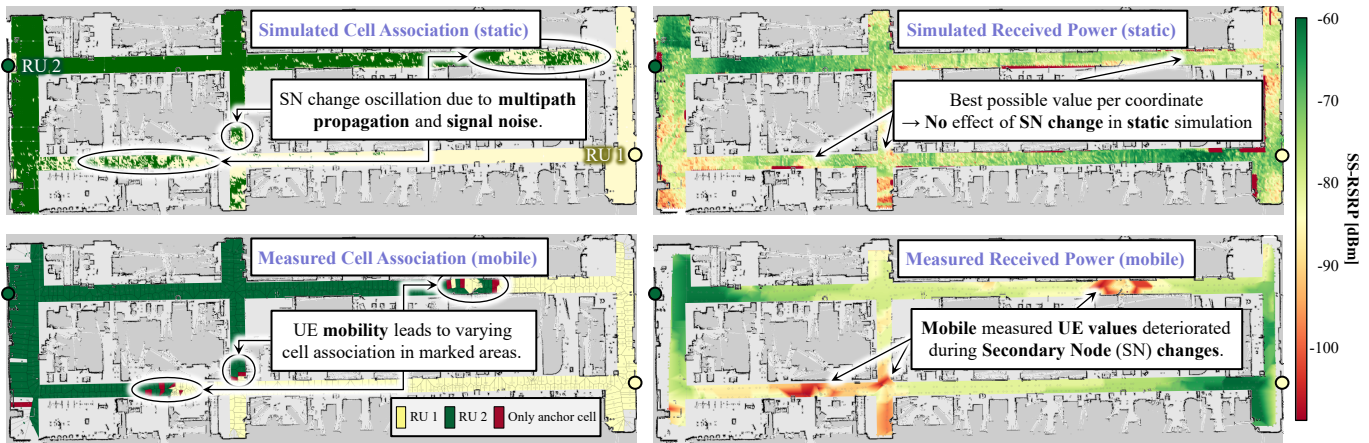


Fig. 3: Comparison of simulated and mobile measured mmWave cell association as well as SS-RSRP for horizontal UE alignment.

A. Mobile User Baseline Performance

The REMs used to investigate the baseline performance of single users in all corridors is shown in Fig. 3. It compares the simulated and measured SN assignments as well as SS-RSRP, respectively. The simulation results were obtained using *Wireless InSite* [13] ray tracing within an abstracted 3D model of the entire radio environment. In addition to sculpting the objects, the antenna characteristics of the RUs and UEs were also taken into account in order to model the radio propagation as realistically as possible.

Compared to previous measurements in [2], the results show no disconnections, as the multi-cell mmWave deployment provides wide area coverage. The simulated and measured SS-RSRP values are comparable in that the connectivity in front of each mmWave RU is best, but differs in the transition areas between the two cells where SN changes occur. There are two reasons for this: firstly, static UE positions are assumed during ray tracing calculations, and secondly, the radio propagation of each cell is simulated independently. However, overlaying these simulation results and evaluating which cell per coordinate provides the better connectivity at the receiver gives an idea of why SN switching oscillations occur in reality during mobile measurements, as the measured cell association (based on NR-PCID) shows. Since the existing network decides on an SN change based on a single signal strength value, and the channel quality can change several times within a small area due to small-scale fading effects, such as multipath propagation and signal noise, the mobile STING repeatedly switches between the two RUs as it passes through SN change areas. This results in deteriorated measurement values within the three circled areas, which will be examined in more detail in the following.

The baseline performance reveals that the multi-cell mmWave deployment provides consistent coverage without interruptions, with the best connectivity in close proximity to each RU. However, due to the presence of cell change areas, multiple SN switches occur at the marked locations both in simulation and during measurements, resulting in short-term performance degradation.

B. Effects of UE Alignment and Environmental Changes

To analyze the effects of UE alignment and environmental changes, we refer to the results of Fig. 4, where NR-PCID and DL data rate of mobile STING are compared with each other in three different scenarios. The difference between scenario (1) and (2) is the UE orientation, which changes from horizontal (towards the ceiling) to vertical (eastwards). The corresponding NR-PCID REMs show that the vertical orientation causes the SN change areas to shift and at the same time reduces the oscillation between both cells, especially in the southern corridor. The reason for this is the eastward orientation towards RU 1, through which the connection to RU 2 only becomes more effective when the mobile STING is no longer in LOS of the first cell. This explicit cell association is preferable to multiple SN changes, as UE connectivity is affected less often. In the northern corridor, it is noticeable that the UE at the eastern end of the aisle is already connected to cell 2 via a wall reflection, before it is temporarily connected to RU 1 as it moves toward the center of the corridor. In this region, the SN change oscillation is not compensated by the vertical alignment, since the UE is not located in LOS of either cell due to its orientation. The comparison of the DL data rate in (1) and (2) reveals that the performance in the southern corridor can be improved due to the vertical alignment and the resulting reduced oscillation between the two RUs. In contrast, the throughput in the northern aisle in front of RU 2 deteriorates by approximately 100 Mbit/s compared to the horizontal orientation, as there is no direct LOS path to the UE's antenna elements. The fact that the performance of the UE in this area is nevertheless comparatively high despite the misalignment to the Base Station (BS) is due to the predominantly metallic environment, which offers many reflection surfaces and can thus contribute constructively to connectivity.

Next, from scenario (2) to (3) with the same vertical UE alignment, the orange-colored crane (cf. Fig. 4) is moved from its central position so that it is 3 m in front of RU 1, which has severe effects on the southern corridor. The SN change area shifts again, as the connection to RU 1 at the western end of the southern corridor has been degraded by the shadowing of the

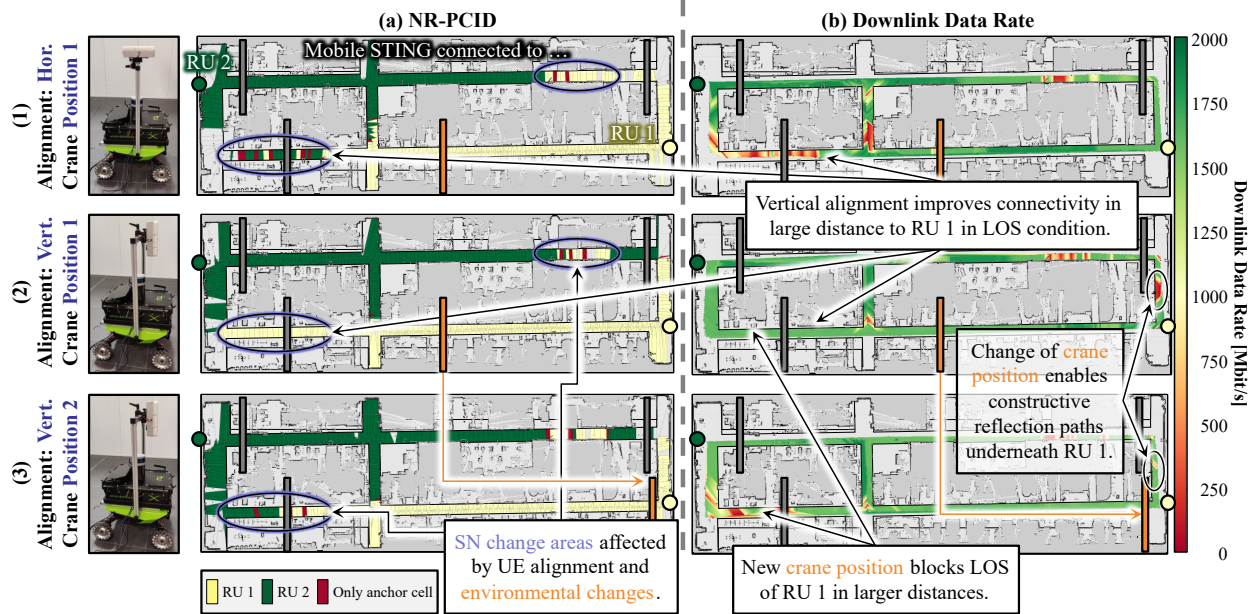


Fig. 4: Effects of UE alignment [(1) to (2)] and environmental changes [(2) to (3)] on network performance shown by (a) NR PCID and (b) DL data rate.

metal crane, resulting in a lower DL data rate. In contrast, the throughput at the eastern end of the hall increases, which is due to new reflection paths created by the modified crane position.

The UE Physical Uplink Shared Channel (PUSCH) transmit power is shown for the same scenarios in Fig. 5. During the transition from (1) to (2), it becomes evident, that the end device is attempting to compensate for the degraded connectivity underneath the RUs caused by the vertical alignment with a higher transmission power. Apart from the close proximity of both cells, the UE transmit power REM illustrates that the vertical alignment leads to an increased energy efficiency at the UE on average. While the mean UE PUSCH transmit power for horizontal alignment is 0.2 dBm, the vertical orientation improves it to an average of -0.25 dBm. With the changed crane position from scenario

(2) to (3), the UE transmit power REM indicates that the blockage affects the whole aisle, as the UE tries to compensate for the degraded channel conditions with automatic transmit power control. The average UE PUSCH transmit power thus increases to 0.3 dBm compared to (2).

For a more detailed analysis of the UE's alignment, additional measurements were performed in which the mobile STING unit drove along the aforementioned trajectory with two different orientations: vertically oriented towards the RU and horizontally towards the roof of the measurement environment. The corresponding received power results are displayed in Fig. 6 as probability density function and the mean value of the respective measured SS-RSRP values. The values of both alignments are analyzed once for the measurements throughout the entire hall as well as only from the southern corridor in LOS of RU 1.

The orientation of the mobile STING's antenna elements towards the ceiling shows the widest distribution. The reason for this is the steepening angle between the cell's and UE's antenna elements as the distance to the RU increases. Due to the limited beam forming capabilities of the UE, the connectivity to the RU decreases. When comparing the values of the southern corridor with those of the entire hall, it is noticeable that the distribution hardly changes, which indicates that the horizontal alignment leads to comparable connectivity in both corridors.

As expected, the vertical orientation in the direction of the mmWave RU 1 leads to the highest received power values being measured in the southern corridor. As the antenna's directivity can be utilized by both the UE and the cell, the connectivity can be improved due to the increase in antenna gains. The average received power rises by 10.30 dB to -69.14 dBm compared to the horizontal orientation. The measured values for the entire hall are also on average

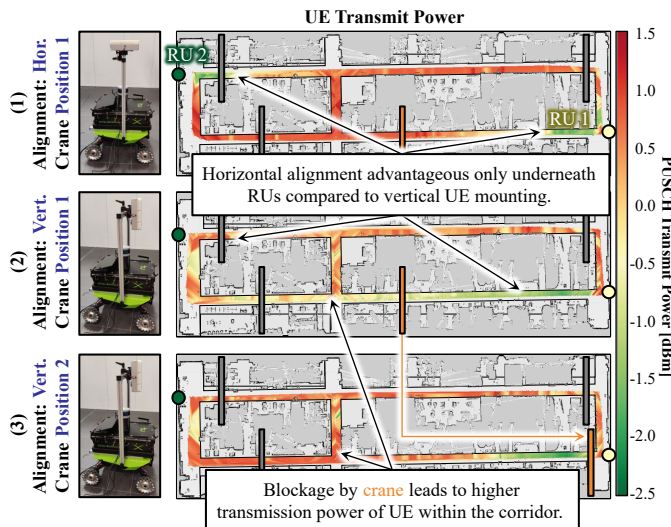


Fig. 5: UE PUSCH transmit power for varying UE alignments [(1) to (2)] and crane positions [(2) to (3)].

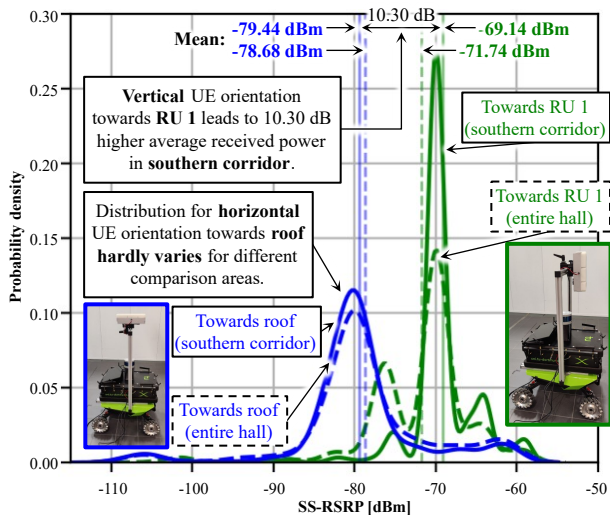


Fig. 6: Impact of UE orientation on received power distribution throughout the entire measurement environment and along the southern corridor.

6.94 dB higher with the vertical orientation than with the horizontal alignment, which is surprising at first, as the UE in the northern corridor is oriented away from RU 2. Such comparatively good received power values can be attributed to the metallic radio environment, as constructive reflection paths can enable good connectivity even in NLOS conditions.

In summary, UE alignment has a significant impact on application performance and connectivity. It can be assumed that a position-dependent, intelligent orientation of the UE would perform best, as it takes advantage of all orientations. The described constructive effect of the metallic radio environment also confirms that intelligently selected or created reflection paths can improve connectivity in challenging radio conditions. The results of the environmental changes prove their major impact on radio propagation. Therefore, in highly dynamic production environments, it is necessary to ensure that large movable obstacles are taken into account during network planning and that such changing conditions are compensated for by the network, as it is the case in the network under consideration.

C. Multi-User and Load Analysis

While the mobile device was the only user of the network in the aforementioned studies, six additional static STING units are now deployed to examine network resource management and the impact of the additional load on all devices. For this purpose, the static devices are placed in front of RU 2 (cf. Fig. 2), while the mobile robot platform follows the previously introduced route. In Fig. 7, the recorded UL data rate of the mobile STING is shown as REM and also as a line plot combined with its cell association as background color and the aggregated throughput of all UEs connected to RU 2. Since only RU 2's resources are fully occupied by the static devices, the mobile STING's performance is initially unaffected by the additional load when moving from waypoints A to C while connected to mmWave cell 1. The UL data rate of the single-

user in this area is at a comparatively high level of over 400 Mbit/s, but also fluctuates due to mobility.

Only at the transition from C to D does the mobile user switch to cell 2. Subsequently, the aggregated throughput of RU 2 drops briefly before the system redistributes the resources to now one mobile and six static users, resulting in an aggregated throughput of 320 Mbit/s again. Compared to RU 1, where the full bandwidth is available to the single mobile user, the UL data rate of the mobile STING now drops to an average of 50 Mbit/s, which is attributed to the competing devices connected to the loaded cell. As soon as the robot switches back to the first cell at the transition from D to C, the mobile STING's data rate increases to an average of 400 Mbit/s again due to more unoccupied resources. Shortly before exiting the cell, the aggregated throughput in RU 2 rises sharply, which is due to a synchronization problem between the measured values of the cell and the mobile STING.

Around waypoint F, the mobile STING is still connected to RU 1. However, the connectivity between UE and the cell in this area is severely degraded due to the Obstructed Line-of-Sight (OLOS) and NLOS conditions, which reduces the reception and the UL data rate at the end device. At the same time, the throughput of the static UEs in RU 2 also falls, which is due to decreasing Modulation and Coding Scheme (MCS) values measured at the mmWave cell. This reduction may be caused by interference of the mobile STING. After another SN change has taken place at the transition from F to D, the previously described observation is repeated again in the area of RU 2.

The results of this study demonstrate the impact of mobility within a multi-cell network on the performance of all connected devices. Concurrently, the significance of responsive radio resource management and adequate capacity planning becomes evident, as these factors are critical for maintaining stability and ensuring a consistently high QoS throughout the radio environment, even under dynamic conditions caused by user mobility and varying network demands.

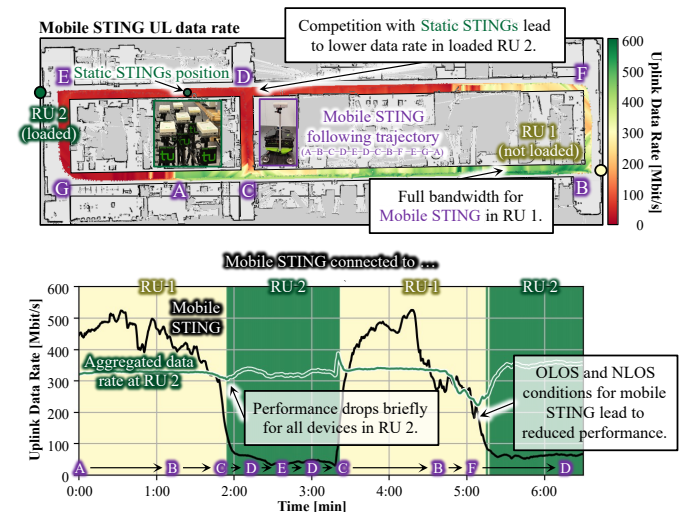


Fig. 7: Multi-load scenario: Site-specific UL data rate of mobile STING with six active static STINGs connected to RU 2.

V. CONCLUSIONS AND OUTLOOK

In this work, we have evaluated the performance of a multi-cell mmWave network in a dynamic industrial environment where one mobile and several static STING devices are deployed for monitoring and stress testing. For the corresponding measurement series, we focused on end device mobility to visualize baseline network performance and investigate the influence of different UE alignments, environmental changes as well as load scenarios. The mobile single-user results indicate full coverage of the accessible aisles within the radio environment, which is a major improvement over previous measurements where only one mmWave RU was deployed within the same radio environment. Furthermore, the conducted baseline measurements indicate clearly how the necessary Secondary Node (SN) changes can temporarily affect the QoS. We also confirmed the influence of UE orientation and environmental changes on the three determined SN change areas as well as on the end device's throughput and transmission power. These results, in conjunction with a more detailed orientation study, emphasize the benefits that a location-specific alignment of mmWave-enabled end devices can have on their performance, energy efficiency and connectivity. Lastly, the resources of one of the two RUs were occupied using static multi-users, whilst the mobile measurement unit was utilized to ascertain the impact of high load as well as mobility on its own performance and that of all connected devices within the multi-cell network. Therefore, the importance of responsive radio resource management and adequate capacity planning is highlighted, as they are crucial to ensure stability and consistently high QoS for multiple mobile devices within a network.

Building on these findings, we will conduct detailed mobility studies in a controllable measurement environment in our future work. In this context, a robotic arm will be used to generate reproducible trajectories, maneuvering the associated UE with different speeds and orientations while connected to a multi-cell network. In conjunction with an energy model grounded in laboratory measurements, the objective is to develop optimization strategies to achieve an efficient trade-off between UE performance and energy efficiency, especially in challenging radio conditions such as in NLOS areas. This procedure can be carried out for different end devices in order to be able to compare their performance and mobility support with each other.

Moreover, the performance evaluation of the multi-cell network can be extended by further KPIs, such as latency and jitter, to investigate their sensitivity to SN switches, UE alignment and environmental changes. In addition, the introduction of intelligent reflectors to the radio environment in challenging radio conditions offers promising potential to counteract connectivity degradation due to obstacles as seen in [2]. Subsequent investigations will determine to what extent SN changes are influenced and, if necessary, stabilized by the resulting Beyond Line-of-Sight (BLOS) links.

ACKNOWLEDGMENT

This work has been funded by the German Federal Ministry of Education and Research (BMBF) in the course of the 6G-ANNA project under grant no. 16KISK101 and the 6GEM Research Hub under the grant no. 16KISK038 as well as by the Ministry of Economic Affairs, Industry, Climate Action, and Energy of the State of North Rhine-Westphalia (MWIKE NRW) along with the Competence Center 5G.NRW under grant no. 005-01903-0047.

REFERENCES

- [1] J. M. Jornet, N. Yang, R. Nichols, S. Nie, C. Huang, and R. K. Mallik, "Terahertz communications and sensing for 6G and beyond: How far are we?" *IEEE Wireless Communications*, vol. 31, no. 1, 2024.
- [2] M. Danger, C. Arendt, H. Schippers, S. Böcker, M. Muehleisen, P. Becker, J. B. Caro, G. Gjorgjievska, M. A. Latif, J. Ansari, N. Beckmann, N. König, R. Schmitt, and C. Wietfeld, "Performance evaluation of IRS-enhanced mmWave connectivity for 6G industrial networks," in *2024 IEEE International Symposium on Measurements & Networking (M&N)*, 2024.
- [3] C. Arendt, M. Patchou, S. Böcker, J. Tiemann, and C. Wietfeld, "Pushing the limits: Resilience testing for mission-critical machine-type communication," in *IEEE Vehicular Technology Conference (VTC-Fall)*, 2021.
- [4] M. Giordani, M. Mezzavilla, S. Rangan, and M. Zorzi, "Multi-connectivity in 5G mmWave cellular networks," in *2016 Mediterranean Ad Hoc Networking Workshop (Med-Hoc-Net)*, 2016.
- [5] 3GPP Technical Report (TR) 37.340 V18.3.0, "TSG RAN; E-UTRA and NR; multi-connectivity; overall description; stage 2 (release 18)," 2024.
- [6] V. Ayadurai, R. Narayanan, and B.-E. Olsson, "Experiments with industrial robotics systems over an indoor 5G-NSA mmWave deployment," in *Joint European Conference on Networks and Communications & 6G Summit (EuCNC/6G Summit)*, 2023.
- [7] A. Ramírez-Arroyo, M. López, I. Rodríguez, T. B. Sørensen, S. Caporal del Barrio, J. F. Valenzuela-Valdés, and P. Mogensen, "A study of FR2 radio propagation with focus on mobility management in an industrial scenario," in *17th European Conference on Antennas and Propagation (EuCAP)*, 2023.
- [8] A. Tarrías, S. B. Damsgaard, M. López, T. B. Sørensen, P. E. Mogensen, S. Fortes, and R. Barco, "Beam switching in mmWave 5G: Evaluation in a realistic industrial scenario," *IEEE Access*, vol. 12, 2024.
- [9] J. Li, Y. Niu, H. Wu, B. Ai, S. Chen, Z. Feng, Z. Zhong, and N. Wang, "Mobility support for millimeter wave communications: Opportunities and challenges," *IEEE Communications Surveys & Tutorials*, vol. 24, no. 3, 2022.
- [10] J. Liu and H. Zhang, "Dynamic aerial reconfigurable intelligent surface aided multi-cell multi-user communications," *IEEE Transactions on Wireless Communications*, vol. 23, no. 11, 2024.
- [11] J. Biosca Caro, J. Ansari, B.-E. Olsson, N. Beckmann, N. König, R. H. Schmitt, F. Popp, and D. Scheike-Momberg, "Empirical performance evaluation of 5G millimeter wave system for industrial-use cases in real production environment," *Electronics*, vol. 14, no. 3, 2025.
- [12] iPerf - The TCP, UDP and SCTP network bandwidth measurement tool. [Online]. Available: <https://iperf.fr/>
- [13] Wireless InSite - 3D wireless prediction software. [Online]. Available: <https://www.remcom.com/wireless-insite-em-propagation-software>